

BJP

Bangladesh Journal of Pharmacology

Research Article

$1\alpha,25$ -Dihydroxyvitamin  $D_3$  reduces uropathogenic *E. coli* persistence in bladder epithelial cells by restoring lysosome acidification

# 1 $\alpha$ ,25-Dihydroxyvitamin D<sub>3</sub> reduces uropathogenic *E. coli* persistence in bladder epithelial cells by restoring lysosome acidification

Hao Yin, Yi Xue, and Xin Wang

Department of Nephropathy, Suzhou Hospital of Integrated Traditional Chinese and Western Medicine, Suzhou, China.

## Article Info

Received: 3 February 2025  
Accepted: 15 March 2025  
Available Online: 25 April 2025  
DOI: 10.3329/bjp.v20i1.79655

### Cite this article:

Yin H, Xue Y, Wang X. 1 $\alpha$ ,25-Dihydroxyvitamin D<sub>3</sub> reduces uropathogenic *E. coli* persistence in bladder epithelial cells by restoring lysosome acidification. Bangladesh J Pharmacol. 2025; 20: 8-15.

## Abstract

This study aimed to examine the effect of 1 $\alpha$ ,25-dihydroxyvitamin D<sub>3</sub> [1,25(OH)<sub>2</sub>D<sub>3</sub>] on the intracellular persistence of uropathogenic *Escherichia coli*. After establishing a cell infection model and conducting drug intervention, methods such as fluorescent probes, Western blot, and qPCR were used. The results showed that 1,25(OH)<sub>2</sub>D<sub>3</sub> (10 nM) reduced the number of persistent *E. coli* (at 12 and 24 hours) (P<0.05), enhanced the acidification of intracellular lysosomes (p<0.05), and up-regulated the expression levels of transcription factor binding to IGHM enhancer 3, ATPase H<sup>+</sup> transporting V0 subunit C, and ATPase H<sup>+</sup> transporting V0 subunit D2 (P<0.05). Therefore, 1,25(OH)<sub>2</sub>D<sub>3</sub> may reduce bacterial persistence by enhancing lysosomal acidification and influencing the expression of these factors. These findings provide ideas for the potential application of 1,25(OH)<sub>2</sub>D<sub>3</sub> in reducing the recurrence rate of infectious diseases.

## Introduction

Urinary tract infections rank among the most widespread infectious diseases globally, with a yearly impact of more than 150 million individuals. Of this patient group, roughly one-quarter contend with recurring infections, and there are cases where some people must endure more than six episodes each year (Timm et al., 2025). The pathogen behind urinary tract infection, urinary tract pathogenic *Escherichia coli* takes the lead the causative agent in over 80% of the cases (Kitagawa et al., 2018). It can persist in the lysosomes within bladder epithelial cells for several months, leading to the recurrence of the infection (Wang et al., 2019).

The acidic environment within lysosomes is crucial for eliminating bacteria. (Hu et al., 2023). When bacteria invade bladder epithelial cells, they can trigger autophagy, which results in their encapsulation by autophagosomes and subsequent delivery to lysosomes

(Miao et al., 2015). *E. coli* can secrete hemolysin A, a substance that interferes with the function of V-ATPase, leading to compromised lysosomal acidification (Naskar et al., 2023). While lysosomes with impaired acidification can get rid of some bacteria through exocytosis, the surviving bacteria take advantage of these malfunctioning lysosomes as shelters, allowing them to persist inside the cells (Wang et al., 2019). Research has shown that correcting lysosomal acidification can considerably decrease the intracellular persistence of *E. coli* (Naskar et al., 2023). 1,25(OH)<sub>2</sub>D<sub>3</sub> can enhance lysosomal acidification, and studies have shown that it plays an important role in regulating the inflammatory response (Jin et al., 2018).

To explore whether enhancing lysosomal acidification can reduce bacterial persistence, experiments were conducted using 1,25(OH)<sub>2</sub>D<sub>3</sub>, and the possible mechanisms by which it affects lysosomal acidification to eliminate bacteria were also investigated.



## Materials and Methods

### Bacterial strains and growth conditions

The *E. coli* strain UTI89 was kindly provided by the Central Laboratory of Nanjing University of Chinese Medicine. Take out the cryopreserved UTI89 strain from the -80°C refrigerator and quickly place it in a water bath at 37°C. Gently shake it to enable rapid thawing. After thawing, a sterile pipette was used to aspirate the bacterial solution and inoculate it into the LB broth medium. Then, place it on a constant temperature shaker at 37°C and incubate it with shaking at a speed of 8.9 x g for 18 hours to promote the resuscitation and growth of the bacterial strain.

### Grouping and bacterial infection of HTB-9 cells

Human transitional bladder epithelial cells (HTB-9,  $5 \times 10^5$  cells) (China, iCell-h232) were placed in RPMI 1640 medium (Gibco, C11875500BT) containing 10% fetal bovine serum (Bdbio, F801-050Hi) and cultured in an incubator at 37°C with 5% CO<sub>2</sub>. Subsequently, the cells were seeded into 24-well plates and randomly divided into three groups: the control group, the *E. coli* group, and the *E. coli* + 1,25(OH)<sub>2</sub>D<sub>3</sub> group. For the *E. coli* + 1,25(OH)<sub>2</sub>D<sub>3</sub> group, 1,25(OH)<sub>2</sub>D<sub>3</sub> (10 nM, MCE, HY-131450) was added to the medium according to a research method (Chan et al., 2022). An equal volume of phosphate-buffered saline was added to the medium of the control group and the *E. coli* group. After 12 hours, following the procedure described by Yin et al. (Yin et al., 2023), the media of the *E. coli* group and the *E. coli* + 1,25(OH)<sub>2</sub>D<sub>3</sub> group were replaced with media containing *E. coli* (with a ratio of bacteria to cells of 100:1).

### Intracellular bacterial counting

The cells were cultured in a complete medium with bacteria for 1 hour, washed thrice using PBS, and then incubated in a complete medium containing 100 µg/mL gentamicin (Aladdin, G647699) for 1 hour to remove extracellular bacteria. After that, the cells were washed

thrice with PBS and cultured in a medium with 100 mM methyl-D-mannoside (Aladdin, M425107) and 10 µg/mL gentamicin for 24 hours. At 2, 12, and 24 hours after infection, lysed the cells with 0.1% triton X-100. The cell lysate was diluted with PBS and then spread on Luria-Bertani agar plates. Incubated the plates in an incubator at 37°C for 12 hours. Taken photos of the plates using a digital camera and analyzed the captured images with ImageJ software to count the number of bacteria (Li et al., 2024).

### Western blot

Washed the HTB-9 cells with pre-cooled PBS. Added RIPA lysis buffer containing protease inhibitors, and lysed the cells on ice for 5 min. Then the cell lysate was transferred to a centrifuge tube, placed on ice for 30 min, and shaken 3 times. Centrifuged at 14,000 rpm for 15 min at 4°C and collected the supernatant to obtain the protein extraction solution. Next, the protein concentration was determined by the BCA method (Mackman et al., 2023). Then, SDS-PAGE electrophoresis was performed. Subsequently, the proteins in the gel were transferred onto a PVDF membrane. Blocked the membrane with 5% BSA at room temperature for 1 hour and then incubated it with the primary antibodies successively (overnight at 4°C) and the secondary antibody (for 1 hour at room temperature). Finally, the membrane was washed, added the ECL luminescent solution, used an imaging system to obtain images and being analyzed the gray values of the bands, to achieve the detection and analysis of the proteins (Wang et al., 2024). The primary antibodies used were lysosome-associated membrane protein 1 (Proteintech, 21997-1-AP, 1:1000), microphthalmia-associated transcription factor (Biodragon, BD-PT2769, 1:1000), transcription factor EB (Biodragon, BD-PT4613, 1:1000), transcription factor E3 (Biodragon, BD-PT4612, 1:1000), and GAPDH (Biodragon, B1034, 1:5000).

### Box 1: LysoTracker red staining

#### Principle

After entering the cell, LysoTracker red is captured and retained by the acidic environment within the lysosome, making the lysosome exhibit red fluorescence under a fluorescence microscope.

#### Requirements

Fetal bovine serum 10% (Bdbio, F801-050Hi); HTB-9 cells; ImageJ software; Incubator (Thermo Scientific Forma 310, USA); Laser confocal microscope (Simple Smart SS-MCS, China); LysoTracker red DND-99 (Yeasen, 40739ES50); Phosphate buffer solution; RPMI 1640 (Gibco, C11875500BT);

#### Procedure

*Step 1:* Prepare the LysoTracker red DND-99 working solution by mixing 1 µL of LysoTracker red DND-99 and 20 mL of

complete culture medium

*Step 2:* The working solution is pre-warmed in a 37°C incubator for 1 hour

*Step 3:* Remove the culture medium and wash three times with phosphate buffer solution

*Step 4:* Add 0.5 mL of the pre-warmed working solution and then incubate at 37°C in a 5% CO<sub>2</sub> incubator for 1 hour

*Step 5:* Remove the working solution and add 0.5 mL of fresh culture medium

*Step 6:* Observe and take image of cells using a laser confocal microscope. The red fluorescence intensity was quantified using ImageJ software.

#### Reference

Chan et al., 2022; Yin et al., 2024

### Immunofluorescence detection

After being washed thrice with PBS, HTB-9 cells were fixed with 4% paraformaldehyde for 20 min. Then, the cells were permeabilized with 0.25% triton X-100 for 10 min thoroughly washed with PBS, and subsequently blocked with 5% BSA at 37°C for 30 min. Following the blocking step, the cells were incubated overnight at 4°C with primary antibodies against lysosome-associated membrane protein 1 (Proteintech, 21997-1-AP, 1:400) and transcription factor E3 (Biodragon, BD-PT4612, 1:150). Washed the cells and incubated with the secondary antibody (Cy3-conjugated goat anti-mouse IgG (H+L), Servicebio, GB21301, 1:500) for 1 hour, followed by treatment with DAPI at 37°C for 10 min. Fluorescence images were captured using a fluorescence microscope. The fluorescence intensity was analyzed using ImageJ software (Zhang et al., 2024).

### RT-qPCR

The MolPure cell/tissue total RNA kit (Yeasen, 19221ES50) was used to extract total RNA from cell samples, ensuring the purity and integrity of the RNA. The extracted RNA was reverse transcribed into cDNA using HS RT SuperMix (Medicalbio, MR0110) to provide a template for the subsequent PCR reaction. The SYBR qPCR Master Mix was prepared according to the instructions. The prepared reaction system was transferred to a PCR reaction plate and placed in a quantitative real-time PCR machine, and an appropriate reaction program was set. After the reaction was completed, GAPDH was used as an internal reference, and the 2- $\Delta\Delta C_t$  method was employed to analyze the data and calculate the relative expression level of the target gene (Srivastava et al., 2023). Primer sequences were as follows:

Transcription factor E3-F: CTCATTATCGTCGGAGCC-ATTG; Transcription factor E3-R: AGTGTGGTCTGGT-ATTCCCTCATA; ATPase H<sup>+</sup>Transporting V0 subunit C-F: GGCATGATCCTGATTCTCATCT; ATPase H<sup>+</sup>Trans-

porting V0 subunit C-R: CTACTTTGTGGAGAGGA-TGAGG; ATPase H<sup>+</sup>Transporting V0 subunit D2-F: GGCTAGAGTGCAATGGCGTGATC; ATPase H<sup>+</sup>Transporting V0 subunit D2-R: CGGGAGGCTGAGGCAGAGAG; GAPDH-F: TGTGGGCATCAATGGATTTTGG; GAPDH-R: ACACCATGTATCCGGGTC-AAT.

### Statistical analysis

The data obtained from the experiment were presented in the format of mean  $\pm$  SEM. Statistical analysis was done using GraphPad Prism 8 (GraphPad Software, USA). A t-test was used to evaluate whether the differences between the data of the two groups were statistically significant. If the p-value was less than 0.05, the difference was determined to be statistically significant.

## Results

### *E. coli* persistence in HTB-9 cells

The results of the cell lysate plating assay indicated that at 2, 12, and 24 hours after bacterial infection, the numbers of intracellular bacteria in the *E. coli* group were 4250.0  $\pm$  528.2, 1566.7  $\pm$  338.6, and 1571.7  $\pm$  199.5 respectively. In contrast, the numbers of intracellular bacteria in the *E. coli* + 1,25(OH)<sub>2</sub>D<sub>3</sub> group were 4383.3  $\pm$  470.8, 538.3  $\pm$  101.9, and 285.0  $\pm$  63.5 respectively. There was no significant difference in the number of intracellular bacteria between the two groups at 2 hours after infection ( $p > 0.05$ ; Figure 1A). However, at 12 and 24 hours after infection, the number of persistent intracellular bacteria in the *E. coli* + 1,25(OH)<sub>2</sub>D<sub>3</sub> group decreased significantly ( $p < 0.05$ ; Figures 1B, C).

### 1,25(OH)<sub>2</sub>D<sub>3</sub> enhances lysosomal acidification in *E. coli*-infected HTB-9 cells

Western blot analysis showed no significant difference in the expression level of lysosome-associated mem-

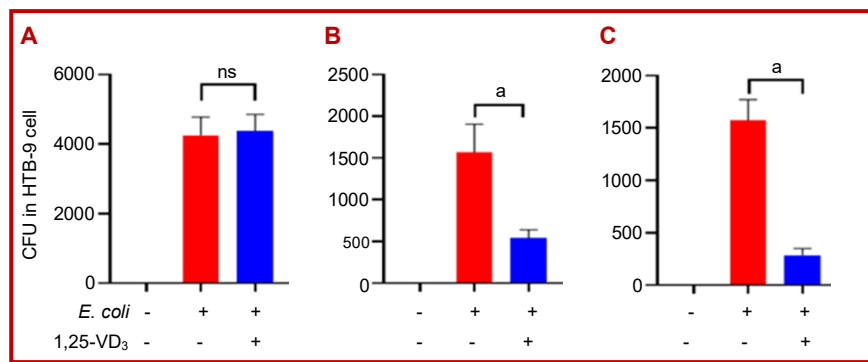


Figure 1: Effect of 1,25(OH)<sub>2</sub>D<sub>3</sub> (1,25-VD<sub>3</sub>, 10 nM) on the intracellular persistent bacterial count of HTB-9 cells infected with *E. coli*. The number of intracellular bacteria in the *E. coli* group and *E. coli* + 1,25(OH)<sub>2</sub>D<sub>3</sub> group 2 hours after infection (A). The number of intracellular bacteria between the *E. coli* group and *E. coli* + 1,25(OH)<sub>2</sub>D<sub>3</sub> group 12 hours after infection (B). The number of intracellular bacteria between the *E. coli* group and *E. coli* + 1,25(OH)<sub>2</sub>D<sub>3</sub> group 24 hours after infection (C). Compared to the *E. coli* group, <sup>a</sup> $p < 0.05$ ; ns = not significant

brane protein 1 between the control group and the *E. coli* group ( $p > 0.05$ ). In contrast, the protein level of lysosome-associated membrane protein 1 in the *E. coli* + 1,25(OH)<sub>2</sub>D<sub>3</sub> group was significantly higher than that in the *E. coli* group ( $p < 0.05$ ; Figures 2A, B). The results of the immunofluorescence staining were consistent with those of the western blot analysis (Figure 2C, D). The results of lysotracker red staining showed that the red fluorescence intensities of the three groups were  $1.0 \pm 0.13$ ,  $0.4 \pm 0.1$ , and  $3.5 \pm 0.4$  respectively. The fluorescence intensity of the *E. coli* + 1,25(OH)<sub>2</sub>D<sub>3</sub> group was

significantly higher than the *E. coli* group ( $p < 0.05$ ; Figures 2E, F).

#### Transcription factor E3 expression in *E. coli*-infected HTB-9 cells

Western blot analysis showed no significant difference in the expression levels of microphthalmia-associated transcription factor among the 3 groups ( $p > 0.05$ ). Compared with the control group, the protein levels of transcription factor EB and transcription factor E3 in the *E. coli* group were lower significantly ( $p < 0.05$ ).

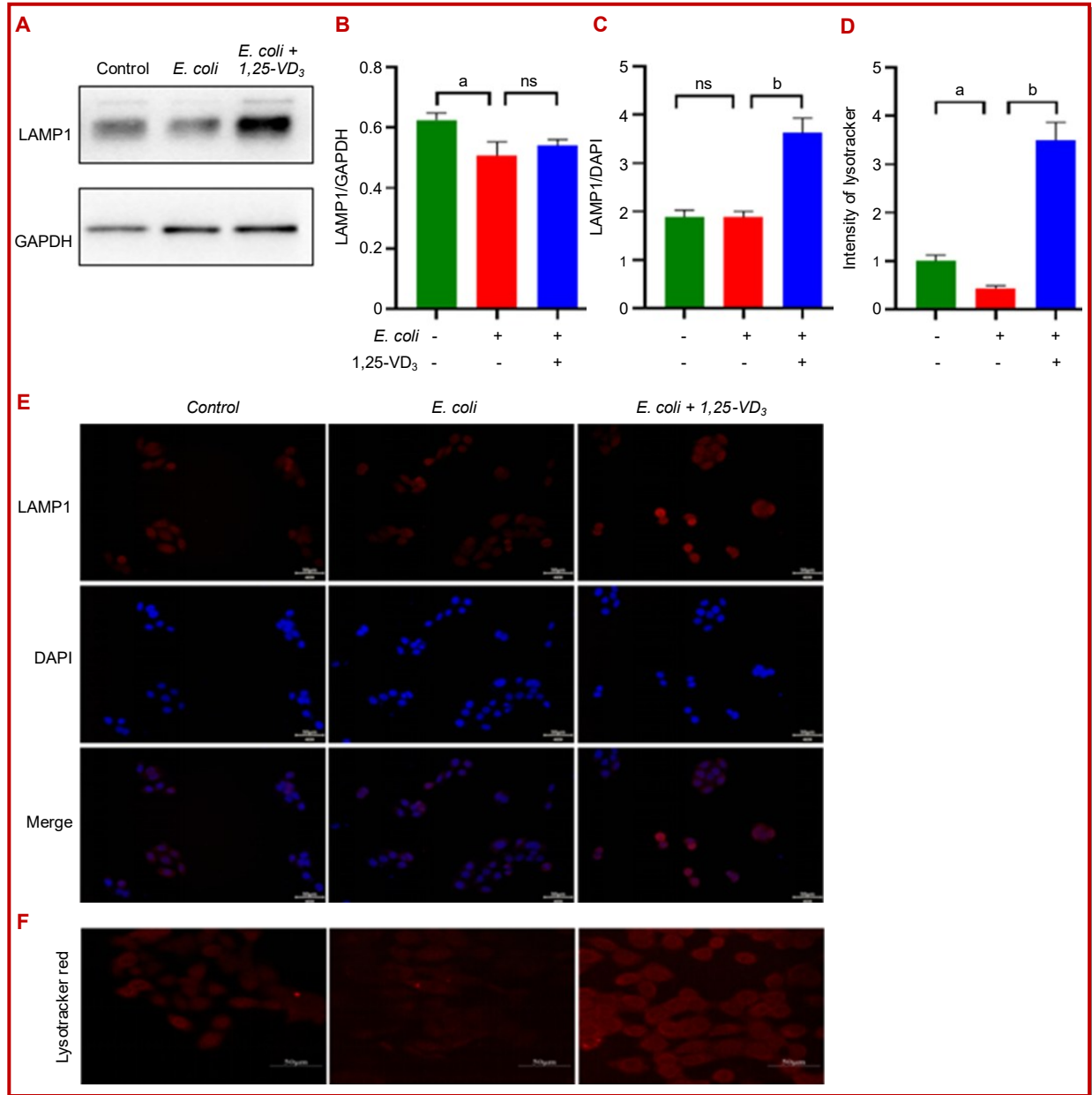


Figure 2: The effect of 1,25(OH)<sub>2</sub>D<sub>3</sub> (1,25-VD<sub>3</sub>, 10 nM) on the lysosomal acidification of HTB-9 cells infected with *Escherichia coli*. The expression results of lysosome-associated membrane protein 1 (LAMP1) were detected by Western blot method (A, B). The fluorescence intensity of lysosome-associated membrane protein 1 was detected by immunofluorescence assay (C, E). The results of the fluorescence intensity detected by lysotracker red staining (D, F). Compared to the control group, <sup>a</sup> $p < 0.05$ ; Compared to the *E. coli* group, <sup>b</sup> $p < 0.05$ ; ns = not significant

The level of transcription factor E3 in the *E. coli* + 1,25 (OH)<sub>2</sub>D<sub>3</sub> group was higher than that in the *E. coli* group

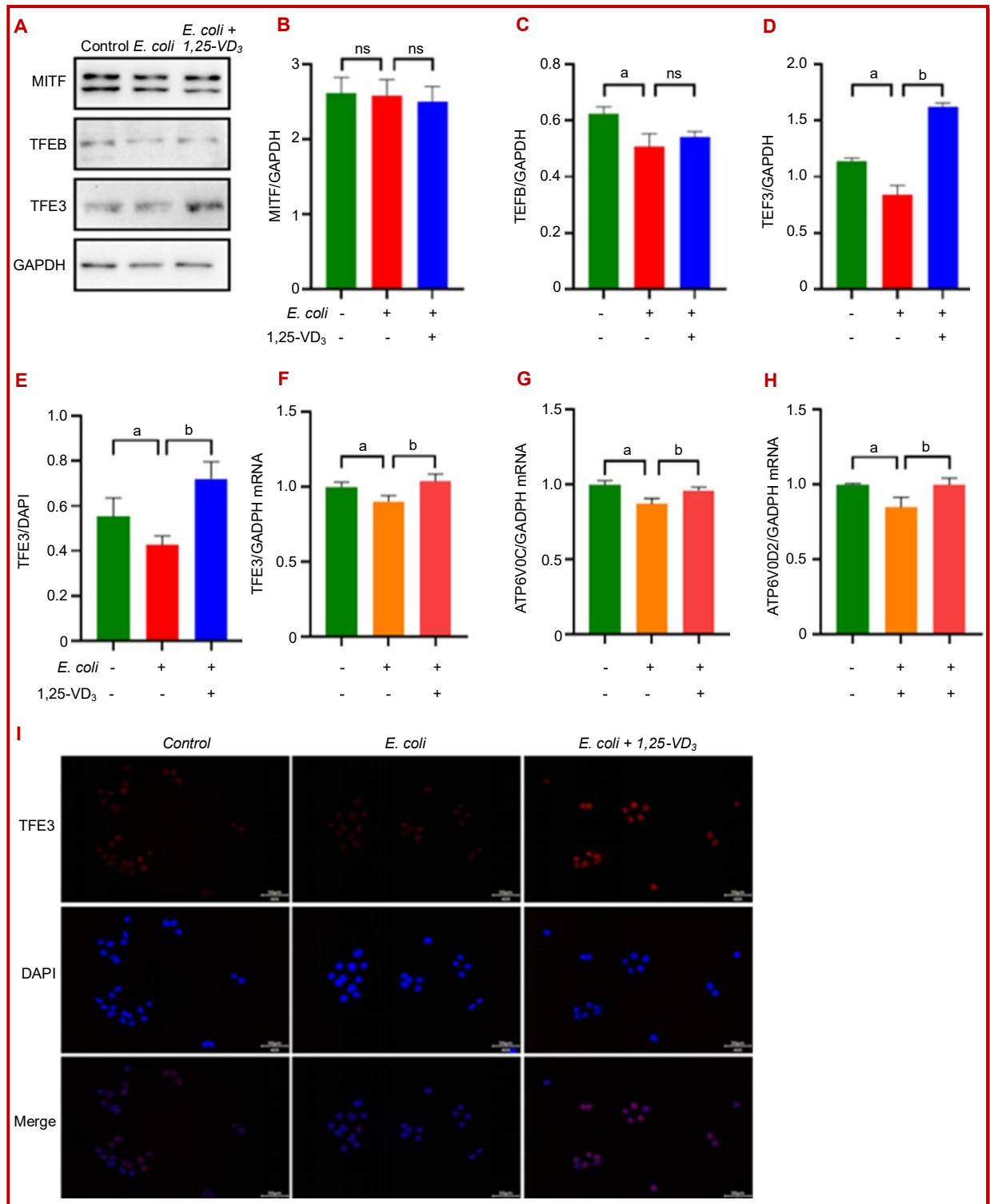


Figure 3: Impact of 1,25(OH)<sub>2</sub>D<sub>3</sub> (1,25-VD<sub>3</sub>, 10 nM) on the MITF/TFE family and V-ATPase subunits in HTB - 9 cells infected with *E. coli*. The expression of microphthalmia-associated transcription factor (MITF), transcription factor EB (TFEB), and transcription factor E3 (TFE3) were detected by western blot (A-D). The mRNA levels of transcription factor E3, ATPase H<sup>+</sup> transporting V0 Subunit C (ATP6V0C), and ATPase H<sup>+</sup> transporting V0 Subunit D2 (ATP6V0D2) were detected by RT-qPCR(F-H). The fluorescence intensity of transcription factor E3 was measured using immunofluorescence assay (E, I). Compared to the control group, <sup>a</sup>p<0.05. Compared to the *E. coli* group, <sup>b</sup>p<0.05; ns = not significant

( $p < 0.05$ ; Figures 3A-D). The fluorescence intensity of transcription factor E3 in the *E. coli* group was significantly weaker than the control group ( $p < 0.05$ ), while the fluorescence signal of transcription factor E3 in the *E. coli* plus  $1,25(\text{OH})_2\text{D}_3$  was significantly more effective than the *E. coli* group ( $p < 0.05$ ; Figures 3E, F). Reverse RT-qPCR analysis compared the control group and the *E. coli* +  $1,25(\text{OH})_2\text{D}_3$  group. The mRNA levels of transcription factor E3, ATPase H<sup>+</sup> transporting V0 subunit C, and ATPase H<sup>+</sup> transporting V0 subunit D2 in the *E. coli* group were significantly lower ( $p < 0.05$ ; Figures 3G, I).

## Discussion

This study shows that  $1,25(\text{OH})_2\text{D}_3$  reduces the persistence of intracellular *E. coli*. It enhances the lysosomal acidification and up-regulates both protein and mRNA levels of transcription factor E3, and V-ATPase subunits. These data suggest that  $1,25(\text{OH})_2\text{D}_3$  alleviates *E. coli* UTI89 persistence by restoring lysosomal acidification through transcription factor E3-mediated transcriptional activation of V-ATPase components.

Bacterial infections pose a significant threat to global health, exacerbated by antibiotic resistance and the persistent nature of certain bacteria (Wang et al., 2023). Persistent bacterial reservoirs are a key factor in the recurrence of chronic infections such as urinary tract infections, tuberculosis, and chlamydia, highlighting the need for innovative strategies to combat microbial dormancy (Niu et al., 2024). Uropathogenic *E. coli*, a major cause of urinary tract infections, serves as a prime example of persistence. Biopsies from patients with recurrent urinary tract infections have shown *E. coli* reservoirs within bladder epithelial cells (Naskar et al., 2023). These intracellular pathogens exploit lysosomal dormancy, where acidic pH-dependent hydrolases are inactivated. *E. coli* is one of several pathogens that disrupt lysosomal acidification: B-coronaviruses induce lysosomal deacidification in HeLa cells, inactivating degradation enzymes (Ghosh et al., 2020). *Clostridioides difficile* triggers abnormal lysosomal activation and inflammation in macrophages (Chan et al., 2022). *Mycobacterium tuberculosis* evades macrophage clearance by disrupting lysosomal acidification (Malik et al., 2025). This highlights the critical role of lysosomal pH homeostasis in host-pathogen interactions. Given the widespread reliance of pathogens on lysosomal deacidification, compounds that restore lysosomal acidification show promise as anti-persistence agents. By reinstating the acidic environment necessary for enzymatic pathogen degradation, these interventions could effectively address recurrent infections.

As a key member of the microphthalmia-associated transcription factor (MITF)/transcription factor E family, transcription factor E3 governs a variety of

cellular processes, such as lysosomal biogenesis, autophagy modulation, metabolic homeostasis, and antimicrobial responses (Pastore et al., 2017). New findings emphasize its vital role in fighting intracellular pathogens. For instance, TRIM27-induced activation of transcription factor E3 boosts autophagic flux, which helps eliminate *Mycobacterium tuberculosis* in host cells. Also, a deficiency in transcription factor E3 impairs macrophage-mediated killing of *Aspergillus fumigatus* conidia (Aufiero et al., 2023). Moreover, transcription factor E3 controls antimicrobial and antiviral responses triggered by interferon- $\gamma$ , lipopolysaccharide, and adenosine receptor pathways (El-Houjeiri et al., 2019). This study, however, sets itself apart from prior ones by involving different cell lines and pathogens.

The V-ATPase, a multisubunit proton pump vital for lysosomal acidification, is often targeted by pathogens to evade host defenses. For example, *Salmonella* hijacks the ATPase H<sup>+</sup> - transporting V0 subunit C to suppress xenophagy in HeLa cells, ensuring its intracellular survival (Xu et al., 2019). *Clostridioides difficile* down-regulates the expression of V0 subunit C, V1 subunit H, and V0 subunit E1 in macrophages, exacerbating inflammatory cascades (Chan et al., 2022). *E. coli* secretes hemolysin A to disrupt V-ATPase activity in bladder epithelial cells, impairing lysosomal acidification and enabling bacterial persistence (Naskar et al., 2023). However, it remains unclear whether *E. coli* affects transcription factor E3 and whether it can influence the levels of V-ATPase subunits.

Studies have shown that  $1,25(\text{OH})_2\text{D}_3$  can not only promote calcium absorption and regulate the immune system but also possess the ability to combat microorganisms. (Fernandes et al., 2022; Kim et al., 2024). The function of  $1,25(\text{OH})_2\text{D}_3$  in combating pathogenic microorganisms is closely related to lysosomal acidification. Some studies have found that it can activate the PDIA3 receptor in gastric epithelial cells, thereby enhancing the degradation ability of lysosomes and effectively eliminating *Helicobacter pylori* (Hu et al., 2019). *Clostridioides difficile* can promote the inflammatory response by disrupting lysosomal acidification, and  $1,25(\text{OH})_2\text{D}_3$  can restore the lysosomal acidification within macrophages to improve this situation. (Chan et al., 2022). However, different from the other studies, this study focuses on the role of  $1,25(\text{OH})_2\text{D}_3$  in enhancing the lysosomal acidification of HTB-9 cells and inhibiting the persistence of *E. coli*.

However, this study has several limitations. Firstly, the experiments were conducted using an HTB-9 cell model, which cannot fully replicate the complex human microenvironment. Secondly, although changes in protein expression levels were observed, the underlying molecular mechanisms remain incompletely understood. Thirdly, the research focused exclusively on *E. coli*, leaving the applicability of these findings to other uropathogens unclear.

## Conclusion

1,25(OH)<sub>2</sub>D<sub>3</sub> significantly enhances lysosomal acidification in HTB-9 cells infected with *E. coli* UTI89, thereby reducing intracellular bacterial persistence. This effect is likely mediated through the up-regulation of transcription factor E3 and two critical V-ATPase subunits: ATPase H<sup>+</sup> transporting V0 subunit C and ATPase H<sup>+</sup> transporting V0 subunit D2-induced by 1,25(OH)<sub>2</sub>D<sub>3</sub>, which collectively restore lysosomal proton-pumping capacity in infected cells.

## Financial Support

This project was supported by the Research Project of the Jiangsu Provincial Society of Traditional Chinese Medicine (No. PDJH2024038). Suzhou Gusu Health Talent Plan Research Program (No. GSWS2022114). Dongwu Health Talent Plan Research Project (No. DWWS2024006). Suzhou Integrated Traditional Chinese and Western Medicine Research Fund (No. SKYD2023243).

## Ethical Issue

Cell lines derived from the expansion of primary cell cultures in vitro were not relevant material, as all the original cells were divided and so the cell line had been created outside of the human body. The storage and use of cell lines created from primary human tissue, for research purposes, did not require ethical approval.

## Conflict of Interest

Authors declare no conflict of interest.

## References

- Aufiero MA, Shlezinger N, Gjonbalaj M, Mills KAM, Ballabio A, Hohl TM. Dectin-1/CARD9 induction of the TFEB and TFE3 gene network is dispensable for phagocyte anti-aspergillus activity in the lung. *Infect Immun*. 2023; 91: e0021723.
- Chan H, Li Q, Wang X, Liu WY, Hu W, Zeng J, Xie C, Kwong TNY, Ho IHT, Liu X, Chen H, Yu J, Ko H, Chan RCY, Ip M, Gin T, Cheng ASL, Zhang L, Chan MTV, Wong SH, Wu WKK. Vitamin D<sub>3</sub> and carbamazepine protect against *Clostridioides difficile* infection in mice by restoring macrophage lysosome acidification. *Autophagy* 2022; 18: 2050-67.
- El-Houjeiri L, Possik E, Vijayaraghavan T, Paquette M, Martina JA, Kazan JM, Ma EH, Jones R, Blanchette P, Puertollano R, Pause A. The transcription factors TFEB and TFE3 Link the FLCN-AMPK signaling axis to innate immune response and pathogen resistance. *Cell Rep*. 2019; 26: 3613-28.
- Fernandes AL, Murai IH, Reis BZ, Sales LP, Santos MD, Pinto AJ, Goessler KF, Duran CSC, Silva CBR, Franco AS, Macedo MB, Dalmolin HHH, Baggio J, Balbi GGM, Antonangelo L, Caparbo VF, Gualano B, Pereira RMR. Effect of a single high dose of vitamin D<sub>3</sub> on cytokines, chemokines, and growth factor in patients with moderate to severe COVID-19. *Am J Clin Nutr*. 2022; 115: 790-98.
- Ghosh S, Dellibovi-Ragheb TA, Kerviel A, Pak E, Qiu Q, Fisher M, Takvorian PM, Bleck C, Hsu VW, Fehr AR, Perlman S, Achar SR, Straus MR, Whittaker GR, de Haan CAM, Kehrl J, Altan-Bonnet G, Altan-Bonnet N. β-Coronaviruses use lysosomes for egress instead of the biosynthetic secretory pathway. *Cell* 2020; 183: 1520-35.
- Hu M, Chen J, Liu S, Xu H. The acid gate in the lysosome. *Autophagy* 2023; 19: 1368-70.
- Hu W, Zhang L, Li MX, Shen J, Liu XD, Xiao ZG, Wu DL, Ho IHT, Wu JCY, Cheung CKY, Zhang YC, Lau AHY, Ashktorab H, Smoot DT, Fang EF, Chan MTV, Gin T, Gong W, Wu WKK, Cho CH. Vitamin D<sub>3</sub> activates the autolysosomal degradation function against *Helicobacter pylori* through the PDIA3 receptor in gastric epithelial cells. *Autophagy* 2019; 15: 707-25.
- Jin W, Cui B, Li P, Hua F, Lv X, Zhou J, Hu Z, Zhang X. 1,25-Dihydroxyvitamin D<sub>3</sub> protects obese rats from metabolic syndrome via promoting regulatory T cell-mediated resolution of inflammation. *Acta Pharm Sin B*. 2018; 8: 178-87.
- Kim JH, Kim K, Kim I, Seong S, Koh JT, Kim N. Stanniocalcin 1 and 1,25-dihydroxyvitamin D<sub>3</sub> cooperatively regulate bone mineralization by osteoblasts. *Exp Mol Med*. 2024; 56: 1991-2001.
- Kitagawa K, Shigemura K, Yamamichi F, Alimsardjono L, Rahardjo D, Kuntaman K, Shirakawa T, Fujisawa M. International comparison of causative bacteria and antimicrobial susceptibilities of urinary tract infections between Kobe, Japan, and Surabaya, Indonesia. *Jpn J Infect Dis*. 2018; 71: 8-13.
- Li X, Jiang L, Zhang S, Zhou J, Liu L, Jin C, Sun H, Wang Q, Liu Y, Pang Y. Uropathogenic *Escherichia coli* subverts host autophagic defenses by stalling preautophagosomal structures to escape lysosome exocytosis. *J Infect Dis*. 2024; 230: e548-58.
- Mackman N, Hisada Y, Park JA. Western blot and immunohistochemical analysis of mouse tissue factor. *Res Pract Thromb Haemost*. 2023; 7: 102249.
- Malik AA, Shariq M, Sheikh JA, Zarin S, Ahuja Y, Fayaz H, Alam A, Ehtesham NZ, Hasnain SE. Activation of the lysosomal damage response and selective autophagy: The coordinated actions of galectins, TRIM proteins, and CGAS-STING1 in providing immunity against *Mycobacterium tuberculosis*. *Crit Rev Microbiol*. 2025; 51: 108-27.
- Miao Y, Li G, Zhang X, Xu H, Abraham SN. A TRP channel senses lysosome neutralization by pathogens to trigger their expulsion. *Cell* 2015; 161: 1306-19.
- Naskar M, Parekh VP, Abraham MA, Alibasic Z, Kim MJ, Suk G, Noh JH, Ko KY, Lee J, Kim C, Yoon H, Abraham SN, Choi HW. α-Hemolysin promotes uropathogenic *E. coli* persistence in bladder epithelial cells via abrogating bacteria-harboring lysosome acidification. *PLoS Pathog*. 2023; 19: e1011388.

- Niu H, Gu J, Zhang Y. Bacterial persisters: Molecular mechanisms and therapeutic development. *Signal Transduct Target Ther.* 2024; 9: 174.
- Pastore N, Vainshtein A, Klisch TJ, Armani A, Huynh T, Herz NJ, Polishchuk EV, Sandri M, Ballabio A. TFE3 regulates whole-body energy metabolism in cooperation with TFEB. *EMBO Mol Med.* 2017; 9: 605-21.
- Pillai-Kastoori L, Schutz-Geschwender AR, Harford JA. A systematic approach to quantitative Western blot analysis. *Anal Biochem.* 2020; 593: 113608.
- Srivastava S, Rasool M. CYT387 restores Th17/Treg cell balance and inhibits mature osteoclast cell formation by regulating SOX-5 signaling in rheumatoid arthritis. *Bangladesh J Pharmacol.* 2023; 18: 138-51.
- Timm MR, Russell SK, Hultgren SJ. Urinary tract infections: Pathogenesis, host susceptibility and emerging therapeutics. *Nat Rev Microbiol.* 2025; 23: 72-86.
- Wang C, Bauckman KA, Ross ASB, Symington JW, Ligon MM, Scholtes G, Kumar A, Chang HW, Twentyman J, Fashemi BE, Xavier RJ, Mysorekar IU. A non-canonical autophagy-dependent role of the ATG16L1T300A variant in urothelial vesicular trafficking and uropathogenic *Escherichia coli* persistence. *Autophagy* 2019; 15: 527-42.
- Wang C, Jin L. Microbial persisters and host: Recent advances and future perspectives. *Crit Rev Microbiol.* 2023; 49: 658-70.
- Wang X, Tang C, Jiang Y, Xue Y, Zhou E. Total flavonoids of *Abelmoschus manihot* ameliorate lipid deposition in HK-2 cells by inhibiting fatty acid uptake mediated by CD36. *Bangladesh J Pharmacol.* 2024; 19: 95-102.
- Xu Y, Zhou P, Cheng S, Lu Q, Nowak K, Hopp AK, Li L, Shi X, Zhou Z, Gao W, Li D, He H, Liu X, Ding J, Hottiger MO, Shao F. A bacterial effector reveals the V-ATPase-ATG16L1 axis that initiates xenophagy. *Cell* 2019; 178: 552-66.
- Yin H, Zhu J, Jiang Y, Mao Y, Tang C, Cao H, Huang Y, Zhu H, Luo J, Jin Q, Jin Q. Shionone relieves urinary tract infections by removing bacteria from bladder epithelial cells. *Cell Microbiol.* 2023; 2023.
- Yin H, Zhu J, Yin J, Xue Y, Wang X. ML098 enhances intracellular bacterial clearance in bladder epithelial cells by activating Rab7 and promoting lysosomal biogenesis. *Bangladesh J Pharmacol.* 2024; 19: 107-13.
- Zhang B, Zhao J, Yin J, Chen J, Xu L. Ginsenoside Rb1 ameliorates neutrophil extracellular traps-induced vascular endothelial damage by suppressing apoptosis. *Bangladesh J Pharmacol.* 2024; 19: 81-87.

**Author Info**

Yi Xue and Xin Wang (Principal contact)  
e-mail: xybft2012@163.com; frogprince417@sina.com